ESRF	**Experiment title:** Oxygen stoichiometry in nanocrystalline CeO_2/Pt under reducing conditions	**Experiment number**: MA- 2533
Beamline: BM23	**Date of experiment**: from: 12 June 2015 to: 16 June 2015	**Date of report**: 20.12.2015 *Received at ESRF:*
Shifts: 12	**Local contact(s)**: Vera Cuartero	

Names and affiliations of applicants (* indicates experimentalists):

Persons who participated in the Experiment at ESRF

* Alexander Guda, Southern Federal University, Russia
* Carlo Lamberti, Southern Federal University, Russia
* Luca Braglia, University of Turin, Italy
* Kirill Lomachenko, Southern Federal University, Russia
* Aram Bugaev, Southern Federal University, Russia

Report:

Pure ceria or Ce-Zr solid solution effectively releases oxygen under lean atmosphere at temperatures above 300 K. This process is accompanied with changing cerium oxidation state from Ce^{4+} to Ce^{3+}, lattice expansion and thus can be monitored with Ce x-ray absorption spectroscopy and x-ray diffraction [1,2]. Ce^{3+} defects have 8 neighbors in the bulk and 6 on the surface with increased Ce-O distances [3]. Pt nanoparticles improve the oxygen release kinetics at low temperature and the catalytic reactions are supposed to take place on the Pt-Ce interface [4]. In this work we use time and space resolved measurements of the CO oxidation reaction in the plug-flow reactor. We thus can address to the elementary steps of the reaction after considering effects related to the sample preparation, design of the in-situ cell, temperature and gas gradients over the catalytic bed [5]. Kinetics measurement will help to understand the role of surface and bulk oxygen in the reaction at different conditions.

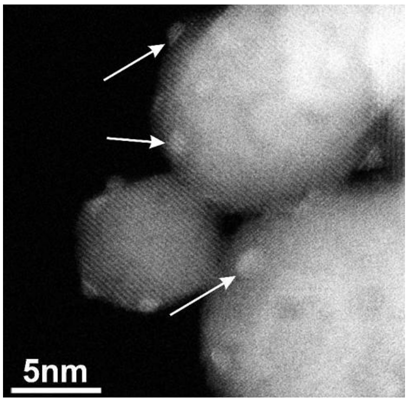

Fig.1 TEM image for CeO_2/Pt nanoparticles under study.

Truncated octahedral CeO_2 nanoparticles were prepared by hydrothermal method. The platinum nanoparticles were deposited on ceria by wetness impregnation by tetraammine platinum(II) nitrate (Aldrich, 99.995%) followed by calcination in air at 674K for 4 h and reduction in 5% H_2 flow at 573K for 4h [3]. The diameter of platinum nanoparticles (shown by arrows in the left figure) is 1.2 (±0.2) nm, and the concentration is 1.5%wt.

We collected the XAS spectra at BM23 beamline of ESRF (Grenoble, France) at Ce K-edge (40470eV). The measurement has been done in transmission mode using a double-crystal monochromator Si (311). Powder sample was introduced within a glass capillary of 1 mm diameter connected to a gas line. Due to high activity of the sample at 150°C the propagation of the front of the reaction through the capillary is clearly visible. It takes several minutes to change to color of the whole powder with a 10 ml/min gas flow speed (see figure 2).

Figure 2. Propagation of the front of the reaction through the capillary at 150°C. CO flow (10ml/min) was switched after O_2 flow. Time interval between successive panels is 1 minute.

We measured the steady XANES spectra at 473K in O_2, afterwards we switched in reducing flow of CO, following the temporal evolution of Ce3+ formation. The data were analyzed with Athena software and then the principal component analysis (PCA) [6] has been done with FitIt software [7]. Similar procedure has been adopted for collecting the two-dimensional XRD patterns (λ=0.3024 Å) which were sensitive to the lattice expansion upon oxygen vacancy formation in ceria.

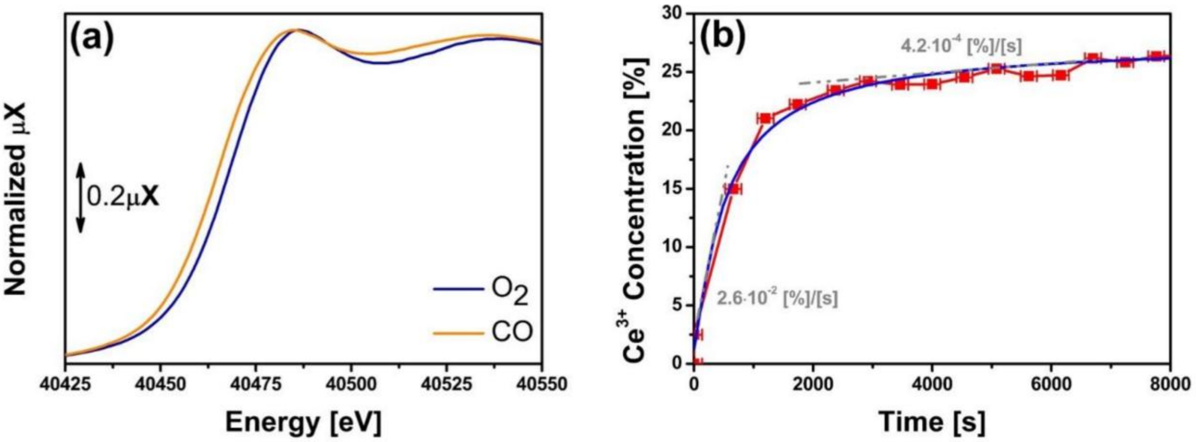

Figure 3. (a) XANES spectra at 423K above Ce K-edge of the CeO_2/Pt nanoparticles in the steady state in O_2 (blue line) and in presence of CO (orange line) after 3 h 15 min of reaction; (b) Temporal evolution of Ce^{3+} formation in reductive condition in function of time at 423K. PCA analysis was performed on the XANES spectra collected at Ce K-edge in CO. We fitted the curve with an exponential function (blue line) and drawn the tangents in grey coloured with their respectively slope values.

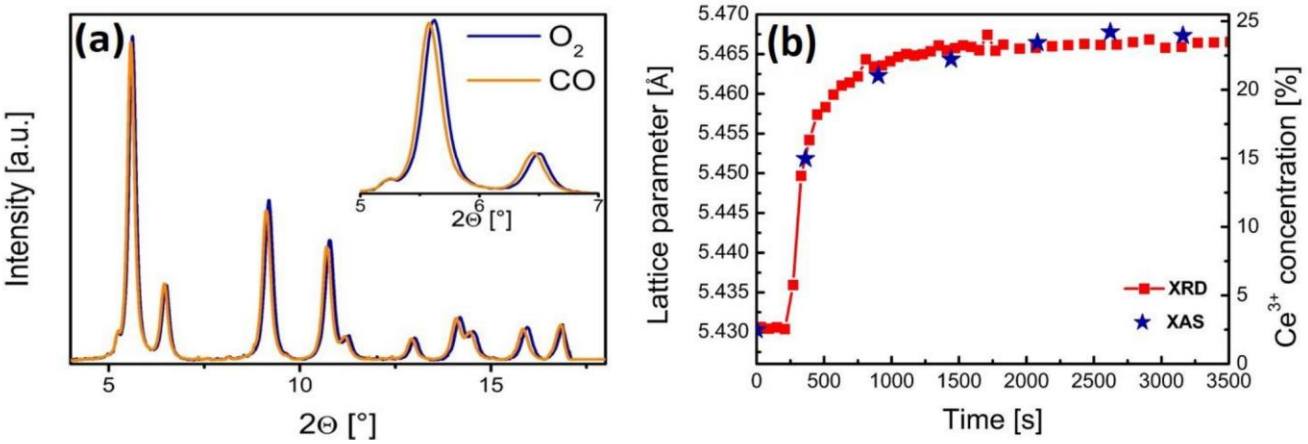

Figure 4. (a) The XRD patterns (λ=0.3024 Å) at 423K are shown in completely oxidized state in O_2 (blue line) and in reduced state in CO gas (orange line). (b) Lattice parameter variation as a function of time (red line) after the CO switching derived from the XRD patterns. The blue star scatter indicate the values of the temporal evolution of Ce^{3+} formation described by XANES spectra previously seen in figure 3b.

In figure 3a we show the Ce K-edge XANES spectra of the sample at the steady state in O_2 (blue curve) and in CO (orange curve) after 3 h 15 min of reaction. In CO the absorption threshold of the XANES spectrum is shifted toward lower energy and the shape of the second peak is shifted to lower energy indicating increase of Ce-O distances. Principal component analysis (PCA) was performed for series of XANES spectra during the CO fluxing and revealed two independent components. We associated the components to Ce^{3+} and Ce^{4+} state and time evolution of Ce^{3+} concentration is shown in figure 3b. The trend of the curve in figure 3b presents a drastic rise until 20% corresponding to the percentage of Ce^{3+} formation in the first 20 min that undergoes to a significant decrease of the rate reaching a plateau at around 25% of Ce^{3+}. Thus the plot in figure 3b can be divided in two regions: region I, which occurs during the first 20 min of flow in CO, where the CO molecules absorbed on Pt surface react with the oxygen provided by the CeO_2 urface with the following reduction of Ce^{4+} atoms. This mechanism yields an increasing of the oxygen vacancies in the local area around Pt nanoparticles and on the surface of ceria, leading a lack of available O atoms for the reaction with CO absorbed on Pt surface. In region II we observed that the rate of Ce^{3+}

formation rapidly decrease, possibly in association with the oxygen migration from the bulk to the surface. We estimated the rate of Ce^{3+} formation in the two regions mentioned before, drawing the two tangents for the respectively parts. The tangent in the region I, reported in figure 3b, presents a slope of 2.6×10^{-2} [%]/[s], conversely the slope achieved in the region II, where the Ce^{3+} formation rate is much slower, is 4.2×10^{-4} [%]/[s].

Cerium forms non-stoichiometric oxides with the fluorite structure. The effect of Ce^{3+} formation can be also supported with the variation of lattice parameter distances, hence we collected powder XRD patterns with the same setup and procedure used previously for XAS experiment. In figure 4a we show the XRD patterns for the steady state of the sample in O_2 (blue line) and in CO (orange line). XRD patterns were collected during the switching to the flux of CO as a function of time, thus following the temporal variation of the lattice parameter. The lattice parameter has been derived for each XRD pattern and shown in figure 2b. Similar trend as observed in XAS was quatified in XRD kinetic profile: fast Ce3+ formation rate in the first 500 s and subsequent slow formation rate during next 2000 s.

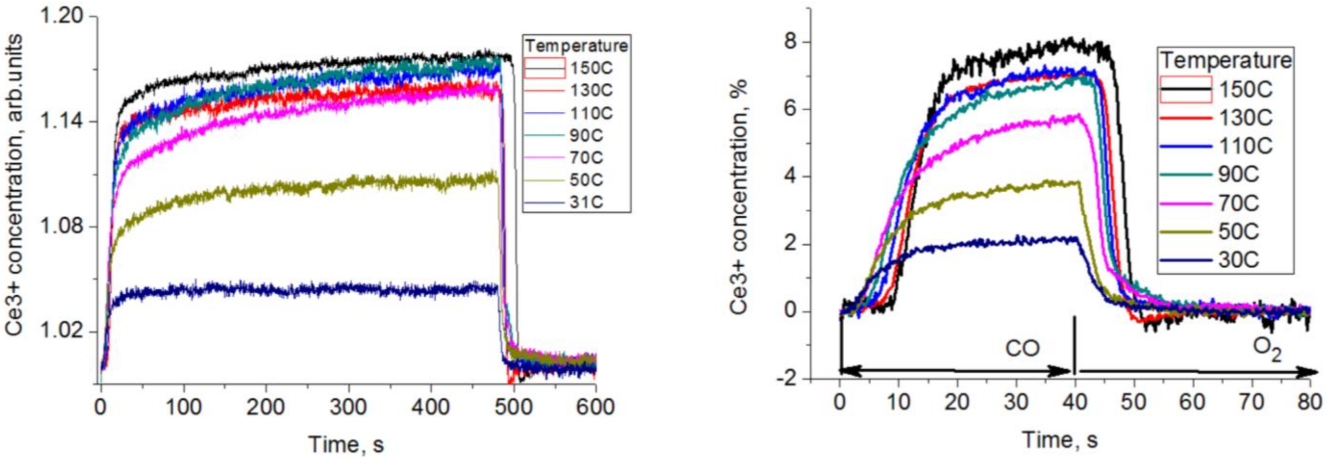

Figure 5. Ce^{3+} formation kinetics obtained from XAS spectra in a single energy point where maximal difference between Ce^{3+} and Ce^{4+} is expected. Left panel shows longer aquisition time with normalized intensity counts while right panel shows shorter aquisition period and intensity counts converted into Ce^{3+} concentration values.

Due to poor statistics at Ce K-edge energy the time required for each XAS spectrum (200eV above the absorption edge) was around 9 min, while for XRD it was 1 minute. In order to analyse faster kinetics we have measured intensity of the XAS spectrum in a single energy point upon O_2/CO switching. Figure 5 shows the obtained concentration profiles as a function of time for different temperatures. We observed the increase of the maximal Ce^{3+} concentration along with temperature and increase of the incubation period (see the delay in the start of the Ce^{3+} formation in figure 5b during first 10 s). Also it is clear that kinetics curve of Ce3+ formation ontained from XAS can't be explained by means of a single exponent. We observe a fast process within first several seconds which is changed by a slow process with a minutes duration.

[1] J. Paier, C. Penschke, and J. Sauer, Chem. Rev. 113, 3949 (2013).
[2] T. Yamamoto, A. Suzuki, Y. Nagai, et.al., Angew. Chem.-Int. Edit. 46, 9253 (2007).
[3] O. V. Safonova et al., J. Phys. Chem. C 118, 1974 (2014).
[4] M. Cargnello, V. V. T. Doan-Nguyen, et.al., Science 341, 771 (2013).
[5] J. D. Grunwaldt, et.al., Phys. Chem. Chem. Phys. 6, 3037 (2004).
[6] Beale A M, Le M T, Hoste S, and Sankar G 2005 Solid State Sci. 7 1141-8
[7] Smolentsev G and Soldatov A V 2007 Comput. Mater. Sci. 39569-74